

Numerical Simulations of As-Extruded Mg Matrix Composites Interpenetrated by Metal Reinforcement

H Y Wang , S R Wang^{*} , X F Yang and P Li

School of Mechanical Engineering, University of Jinan, Jinan, 250022, China

Corresponding email: me_wangsr@ujn.edu.cn

Abstract. The interpenetrating magnesium composites reinforced by three-dimensional braided stainless steel wire reinforcement were fabricated and investigated. The extrusion processes of the composites in different conditions were carried out and simulated by finite element method using the DEFORM-3D software. The results show that the matrix and reinforcement of the composites form a good interfacial bonding and the grains were refined by extrusion and the influence of reinforcement, which are in accordance with the enhanced strength and degraded plasticity. The combined quality between the matrix and reinforcement can be strengthened in extrusion chamber where occurred large strain and suffered intense stress, and the effective stress of the material increases continuously with the increase in extrusion ratio and the decrease in extrusion speed until it reaches a stable value.

1. Introduction

Mg and its alloy are the lightest metallurgical based structural materials with high specific strengths, and therefore they are the most attractive materials in many fields where weight reduction is of prime importance, such as automotive, aerospace and mobile electronics and so on. However, owing to the low strength, the Mg alloy was usually reinforced by particles, whiskers and short or long fibers to form magnesium matrix composites to improve the strength and performance of the materials. In recent years, the reinforcement network skeletons of magnesium matrix composites are tended to make from ceramic, glass, cement, intermetallic and so on[1-4], which would lead the composite materials to exhibit some excellent mechanical properties than the traditional magnesium matrix composites[5]. But the defect is that the interpenetrating composites cannot be further deformed to the required shape due to the brittleness of the reinforcement, so their application is still limited in manufacturing the structural components with the cross section shape of fixed type. If the reinforcement of the composites were made from metal that is the metal matrix composites interpenetrated by metal reinforcement (MIMC) would have a good forgeability and machinability which can be a variety of thermal deformation and Cold deformation. And through the plastic deformation, for example, twin-roll casting (TRC), warm rolling (WR), hot extrusion (HE), torsion straining (TS), reciprocal extrusion (RE) and equal channel angular extrusion (ECAE)[6-8], the combined quality between matrix and reinforcement of the composites can be improved and also the cross-sectional shape of the materials can be changed to meet the requirement. In this study, Mg alloys matrix composites interpenetrated by steel reinforcement (MISC) were manufactured and expected to obtain the excellent mechanical properties attributing to the coordination deformation mechanism of reinforcement with magnesium matrix during deformation[9].



In order to ensure the reliability and safety of subsequent applications, the magnesium matrix composites must be of high quality, especially the combined quality between the reinforcement and matrix of the materials. So the extrusion process of the MISC materials was performed so as to improve the combined quality and the strength of the materials. It is practically impossible to measure stresses and temperatures of the materials in extrusion chamber based on the currently experimental methods. So, in this case, computer simulation based on the finite element method theory (FEM) can play an important role in revealing the evolution and distribution of effective stress, pressure and temperature of the product during the deformation process[10].

In the present works, the fabrication and subsequent extrusion process of the MISC were carried out. The microstructure and texture evolution during deformation was analyzed in detail. And the deformation behaviour of MISC materials during extrusion process were also investigated through finite element methods using a viscoplastic material model. The main objective was to acquire the internal stress of the composites, and the extrusion speed and ratio were used as process variables to evaluate their effects on the extrusion pressures, stresses and temperatures of the extruded product during the extrusion process. The simulation results are looked forward to guide the practical process production and experimentation.

2. Simulation and experimental procedures

2.1. Experimental procedures

The 304 stainless steel (Fe-18Cr-9Ni) wire (diameter as 0.6 mm) was chosen as the reinforcement skeleton materials, and the three dimensional braiding technology was applied to fabricate the skeleton. The AZ31 (Mg-3.31Al-1.05Zn) magnesium alloy were chosen as the matrix alloy. The volume fraction of reinforcement is about 15% which was measured using Archimedes measurements (ASTM C373). The MISC composites were fabricated by using the pressure infiltration technology, and the whole process is protected under argon atmosphere together with the infiltration die. The magnesium alloys were melted at 720°C under an inert atmosphere of CO₂ and SF₆ mixture. After melting, the melt was poured down into the infiltration die where have been placed the reinforcement skeleton in it at the temperatures range of 640-670°C, and then pushing the pressure head. As a result, MISC composites were fabricated successfully. Subsequently the extrusion process was carried out using the extrudate die with a lumen diameter of 40mm, a die half angle of 30° and an extrusion ratio of 16, as shown in Figure 1(a), at a temperature of 350°C under the extrusion speed of 2mm/s. The extrusion billet was machined to a specified diameter of 39 mm before extrusion, the extruded material is quenched to avoid grain growth. Extrusion experiment was performed to illustrate the effects of the compressional stress on the microstructure and texture evolution of MISC materials, and to validate that the material properties can be improved through enhancing the binding force between Mg matrix and the 304 reinforcement.

The microstructure characteristics of MISC material in as-cast and as-extruded state were analyzed by optical microscopy (OM), X-ray diffraction (XRD) and electron back-scatter diffraction (EBSD). The mechanical properties of the MISC materials were tested by tensile tests, and the tensile specimen had a gauge length of 12 mm, a width of 3 mm and a thickness of 2 mm. For comparison, the tests of AZ31 Mg alloy were also carried out. And the tensile tests were conducted at room temperature with a constant speed corresponding to an initial strain rate of $1 \times 10^{-3} \text{ s}^{-1}$, where the angle between the tensile direction and the extrusion direction was 0 deg.

2.2. Simulation parameters and conditions

The FE simulation of MISC materials extrusion process was conducted using the software of DEFORM-3D, a coupled thermo-mechanical commercial FE code, which can be used for non-isothermal simulation. Thermo-elastic-visco-plastic FE code used in this study have both temperature and displacement as their degrees of freedom and could successfully capture the deformation modes

and the specific characteristics of MISC sample extrusion process. In the analysis, a quarter of the geometries of the workpiece and dies were modeled and meshed with tetrahedral elements due to the symmetric boundary conditions as shown in Figure 1(b). The relative mesh density type was applied for the extrusion head and die which were considered rigid but non-isothermal. However, to improve the accuracy and reliability of FE simulation, the workpiece was meshed using absolute mesh density type where the minimum size of an element was 0.8mm. The total number of elements of the workpiece and tooling were given in table 1 Both of these material models neglected the elastic behaviour.

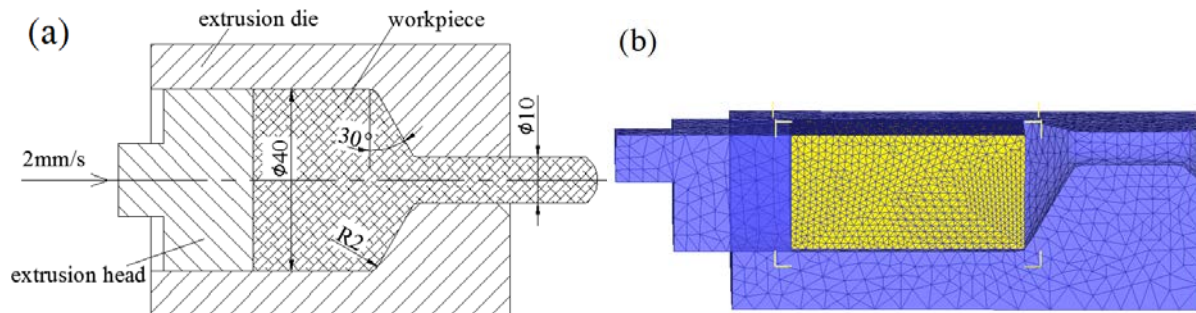


Figure 1. The diagrammatic sketch (a) and initial FE model (b) of the extrusion process

Table 1. The meshing feature of the models

Model	Meshing type	Total number
Extrusion head	relative mesh density type	12000
Extrusion die	relative mesh density type	2500
Workpiece	absolute mesh density type	21660

The material model of AISI-H13 hot-work tool steel in DEFORM-3D software package was chosen for the extrusion head and die. However, a new model should be conducted to match the MISC material because there is no material model employed for it in the software package. The material parameters of MISC as shown in table 2 were obtained from the calculation results based on the parameters of the matrix and reinforcement. The deformation behavior of MISC composites rely on Arrhenius equation,

$$\dot{\epsilon} = A[\sinh(\alpha\sigma)]^n \exp(-Q/RT) \quad (1)$$

where $\dot{\epsilon}$ is the strain rate, σ is the flow stress, A and α are the constant related to materials, n is the strain hardening exponent, Q is the activation energy, R is the gas constant and T is the deformed temperature. Arrhenius equation is the sine hyperbolic law which is a comprehensive and perfect equation combining the power law with the exponential law. And the stress-strain constitutive mode of MISC composites which has been validated in the literature is proposed as,

$$\dot{\epsilon} = 5.047 \times 10^{13} [\sinh(0.02063\sigma)]^{5.355} \exp\left(\frac{-198015}{8.314T}\right) \quad (2)$$

Table 2. The material parameters of MISC

Young's modulus , E / GPa	58.39
Poisson's ratio , ν	0.342
Yield function type	Von Misses
Thermal conductivity λ / $\text{N}\cdot(\text{s}\cdot^\circ\text{C})^{-1}$	108.36
Heat capacity C / $\text{N}\cdot(\text{mm}^2\cdot^\circ\text{C})^{-1}$	1.9876
Thermal expansion α / 10^{-5}	2.016
emissivity	0.172

In order to investigate the effects of the extrusion process parameters on the deformation behaviors of the MISC material, the extrusion processes were simulated under different extrusion conditions via changing the extrusion speed (1, 2, 3, 4 and 5 mm/s) and the extrusion ratio (4, 9, 16, 25 and 36). The processing temperature of the MISC workpiece was set to 350°C, and the tooling and environment were all set to 300°C owing to the poor plasticity of the magnesium matrix at normal atmospheric temperature. The interface heat transfer coefficient between workpiece and tooling was set to 11 $\text{N}\cdot(\text{s}\cdot\text{mm}\cdot^\circ\text{C})^{-1}$ and between workpiece/tooling and air was set to 0.02 $\text{N}\cdot(\text{s}\cdot\text{mm}\cdot^\circ\text{C})^{-1}$ which assumed to be uniform for the entire surface[11]. The shear friction was chosen in this work and choosing 0.3 as the friction factor which was assumed not to vary locally with interface temperature and pressure[12].

3. Results and discussions

3.1. Microstructure characterization

The microstructures and interface characterization of MISC composites are shown in Figure 2. It can be seen that the reinforcement and matrix are anisotropic, interpenetrating and intertwisting. The structure of the reinforcement has a good design ability due to it using the three-dimensional braiding technology. From Figure 2(a), parts of interconnected network structure of reinforcement in longitudinal direction are exposed from the matrix, and only a few of that in transverse direction (black arrow) is exposed., and most parts of it are enwrapped and buried with Mg metal matrix. The matrix and reinforcement form a good interfacial bonding, which is shown in Figure 2(b). The chemical element distributions were examined by Energy Dispersive Spectrometer (EDS) which are shown in Figure 3. The circle reinforcements are Fe which was characterized by blue line, and the Mg matrix was characterized by red line.

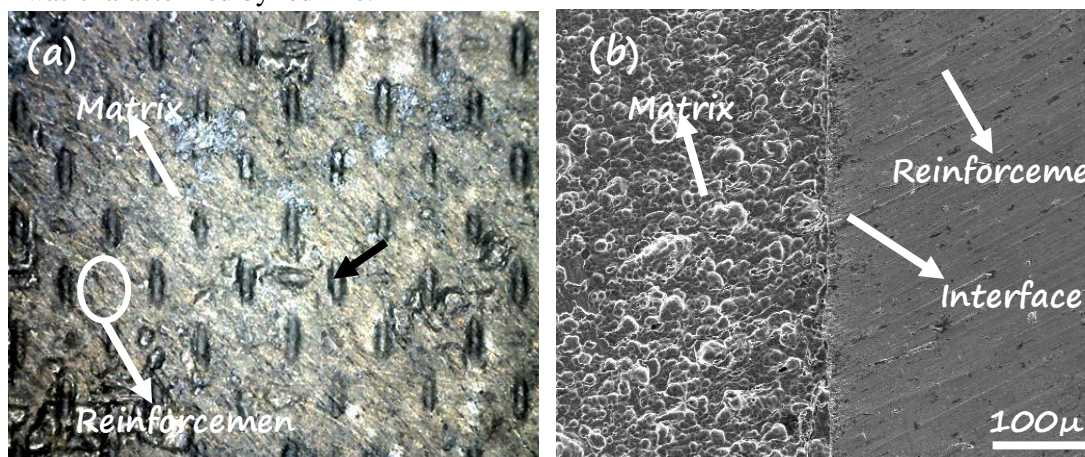


Figure 2. The interpenetrating structure (a) and interface of reinforcement with matrix (b)

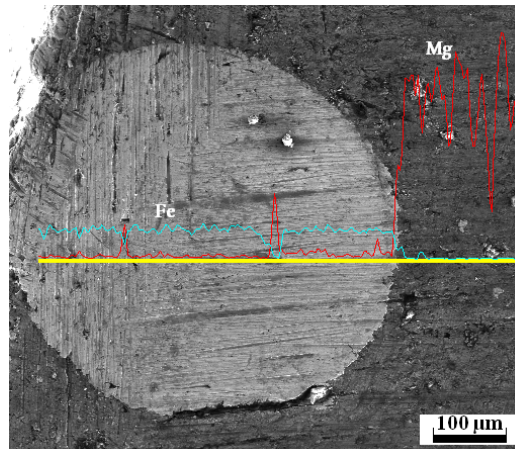


Figure 3. The EDS analysis of MISC composites

Figure 4 shows the Optical Micrographs (OM) (Figure 4(a)) and grain size distributions (Figure 4(b)) of Mg matrix in MISC material as-cast state. The grain size distribution is random which does not follow normal distribution. And the area fraction of small grains with less than 50 μm is about 20%. The large grains with greater than 350 μm are about 12%. It is indicated that the area fraction of grains diameter and distribution don't get any influence from the reinforcement materials. That is, in as-cast state, the grain size and grain distribution of Mg matrix in composites has the same characterization with AZ31 Mg alloy. However, as a comparison of the as-cast state, the microstructure of the as-extruded sample has a larger changes in microstructure characteristics. Figure 5 shows the Field Emission Scanning Electron Microscopy (FESEM) and the grain size distributions of magnesium matrix in MISC material as-extruded state. Due to the accumulated shear strain and dynamic recrystallization during extrusion, the grain size of as-extruded sample became relatively fine (Figure 5(a)), and the grain size distribution follows normal distribution (Figure 5 (b)). The area fraction of small grains with less than 2 μm is about 2%, that of large grains with greater than 30 μm is about 1%. The vast majority of grain sizes are in 10-17 μm , and the average grain size is 14 μm .

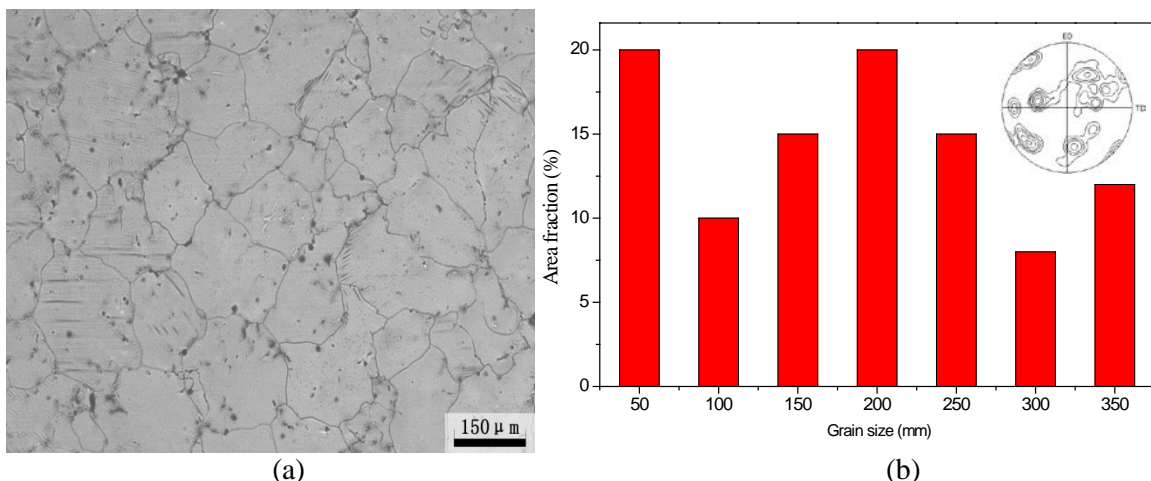


Figure 4. OM (a) and the grain size distributions (b) of Mg matrix in MISC material as-cast state

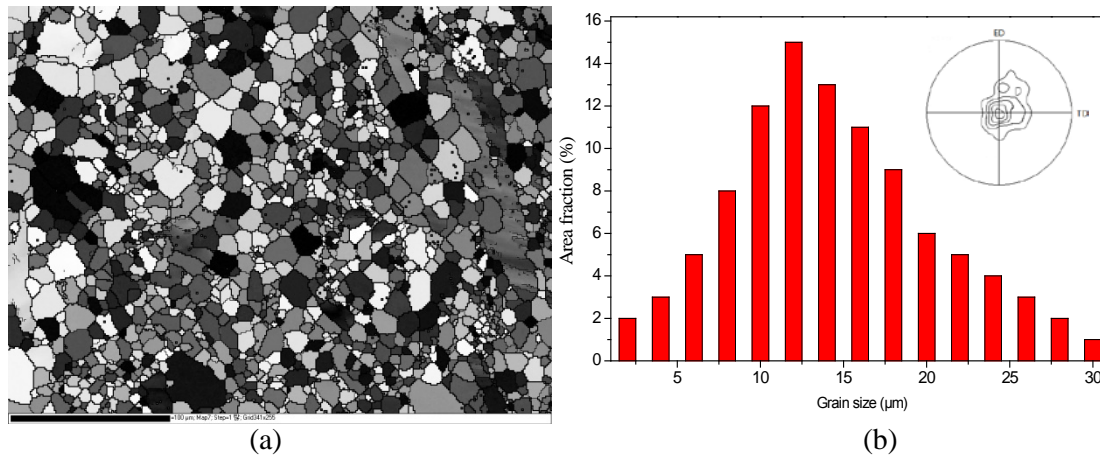


Figure 5. FESEM (a) and the grain size distributions (b) of magnesium matrix in MISC material as-extruded state

The difference of grain refinement and sizes distribution can be further demonstrated by the grain orientation changes of Mg matrix. It is indicated that the $\{0001\}$ basal pole figure for as-cast state shows nearly random distribution which is shown in Figure 4(b). The grain orientation evolution of Mg matrix as extruded state is revealed by EBSD test data from the $\{0001\}$ basal pole figure which is set in Figure 5(b), it is shown that the grain orientation forms a strong peak in the centre of the $\{0001\}$ basal pole figure during extrusion. In MISC material, the stainless steel wires have the highest strength, which cause a larger stress to Mg grains resulting in the basal plane tilted during coordination deformation. Therefore, the dynamical recrystallizations in Mg matrix occur near the strut of the reinforcement. And the room temperature formability of magnesium alloy strongly depends on the influence of the initial crystallographic texture of the basal plane [13]. The basal plane control lead to distinctly improved formability in MISC composites.

3.2. Mechanical properties

Due to the influence of reinforcement materials and the extrusion process, MISC composites exhibit different mechanical properties compared with AZ31 magnesium alloy which are shown in Table 3. The ultimate tensile strength (UTS), yield strength (YS) and elongation (δ) of MISC have a significant improvement compared with Mg matrix alloy (AZ31). The improvement can be summarized as follows as (a) high strength and elongation of the reinforcement itself, (b) good interfacial bonding of reinforcement with matrix caused by extrusion, (c) fine and equiaxed grain during coordination deformation of reinforcement and matrix and (d) effective load transfer from matrix to reinforcement.

Table 3. The YS, UTS and δ of AZ31 Mg and MISC material

materials	YS (MPa)	UTS (MPa)	δ (%)
AZ31	135	240	7
MISC	245	355	13

3.3. Extrusion process simulations

3.3.1. Deformation behaviors of the MISC workpiece during extrusion.

The mesh characteristics and the accompanying stress state of the MISC workpiece during extrusion process were shown in Figure 6. It can be observed that the flow of the billet through the extrusion die may be divided into three stages: upsetting - filling of the extrusion chamber - continuous extruded. And these stages can also be distinguished in the curve of extrusion pressure corresponding to the extrusion displacement which acquisition from the simulation of the extruded at a discharge rate of 2 mm / s and a extrusion ratio of 16 as shown in Figure 7. The extrusion pressure increased sharply in the filling stage and then remained stable in continuous extruded stage. And the fluctuation in the

pressure-displacement curve observed was due to the oscillation of nodes in contact with the extrusion die/head. From the distribution of the effective stress (Figure 6), it is noteworthy that the stress is mainly concentrate on the chamber and the outlet of extrusion die where occurred large strain during extrusion. Corresponding the finer meshes in the chamber indicated the material was subjected to strongly compressive force and the elongated meshes in the outlet illustrated the compressive force in radial direction and tensile force along the axial direction for the material. The combined quality between the reinforcement and matrix of MISC composites could be strengthened in the extrusion chamber where occurred large strain and suffered intense stress, and so as to chieve the interpenetrating and intertwining between them.

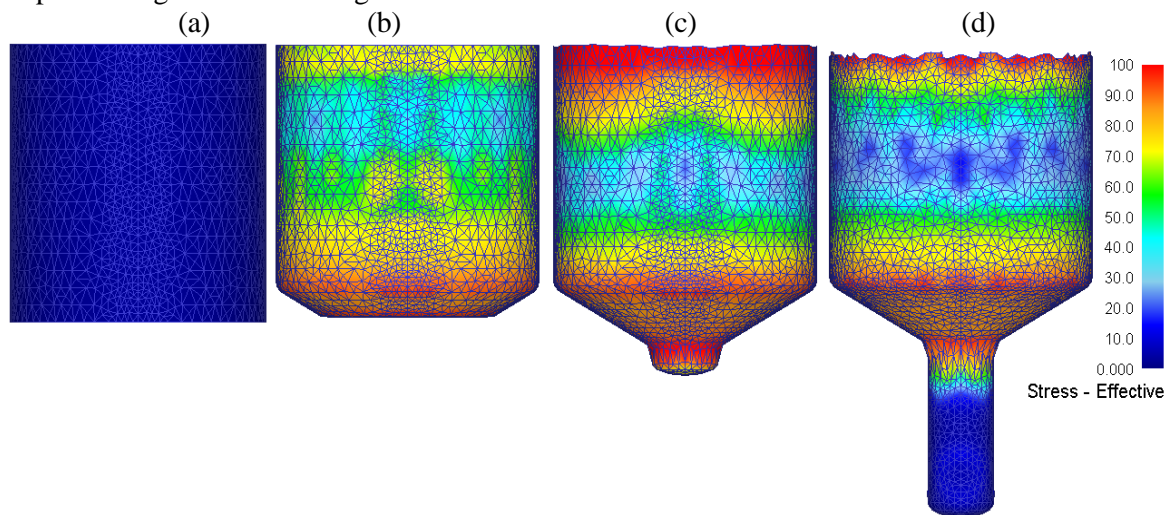


Figure 6. The dynamic extrusion process of MISC: (a)initial state, (b) upsetting, (c) filling of the extrusion chamber and (d) continuous extruded state

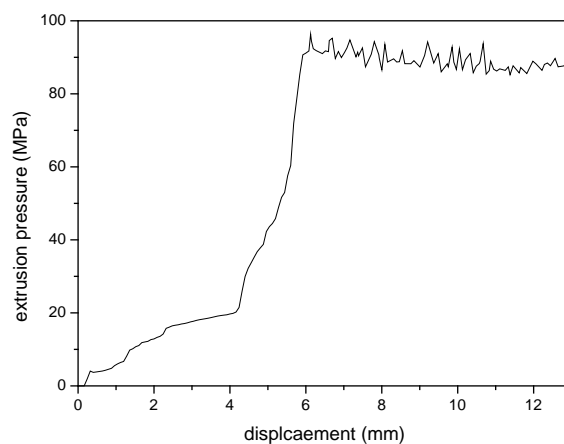


Figure 7. Extrusion pressure evolution obtained from simulation

The deformation characteristics, such as strain distribution, temperature and flow velocity of the MISC workpiece were exhibited in Figure 8 respectively. The material occurred large strain in extrusion chamber and channel due to the combined effects of extrusion pressure and friction as show in Figure 8 (a), and which result in a higher temperature in the outlet of extrusion (Figure 8 (b)) since the energy of the plastic deformation was converted to heat and increase the temperature of the workpiece. However, the increase of the temperature would lead to a decrease on effective stress and

was not conducive to the bonding between the matrix and the reinforcement of MISC composites. The metal flow velocity distribution as shown in Figure 8(c) indicate that the dead metal zone does not obviously in the corners of die due to the chamferings, and it can ensure the smooth and continuous flow of material in extrusion. It also can be seen that the metal in the outlet zone flows much faster than other zones which illustrate the larger strain and stress have been suffered in this zone.

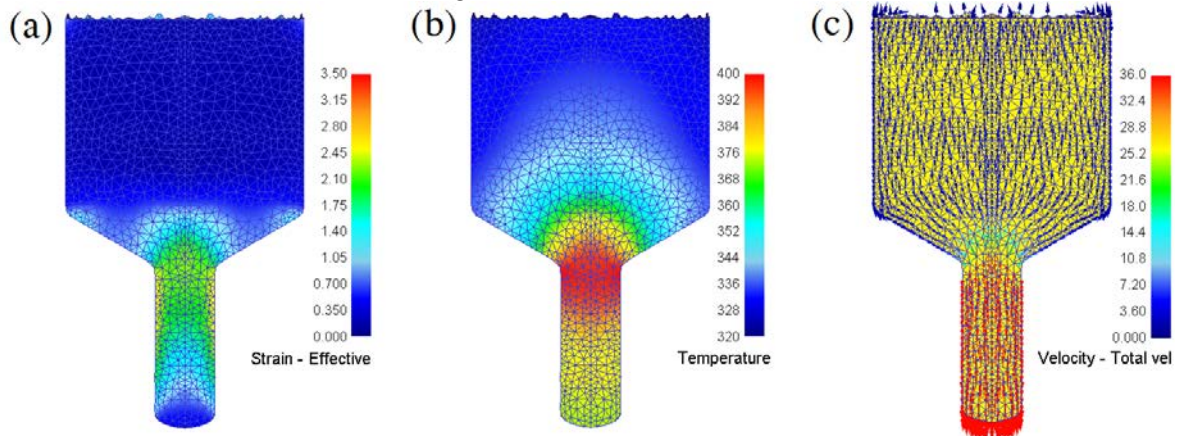


Figure 8. The deformation behaviors of the workpiece during extrusion (a) strain distribution; (b) temperature distribution; (c) metal flow velocity distribution

3.3.2. The influence of the extrusion conditions to the deformation characteristics of MISC material.

The bonding strength between the matrix and reinforcement depends on the value of the effective stress of MISC composites suffered in the deformation region which significantly influenced by extrusion conditions, such as extrusion ratio, speed and temperatures. In this study, all the simulations of extrusion process were carried out under high temperatures due to the poor plasticity of magnesium matrix at room temperature, so only the extrusion speed and ratio were selected as the variable process parameters. In order to observe the difference of the deformation characteristics of composites under different conditions, a series of points in deformation region of material as shown in Figure 9 was tracked. And due to the sizes of the die with different extrusion ratio are different, the tracked points are not the same under different conditions, but always throughout the whole extrusion chamber.

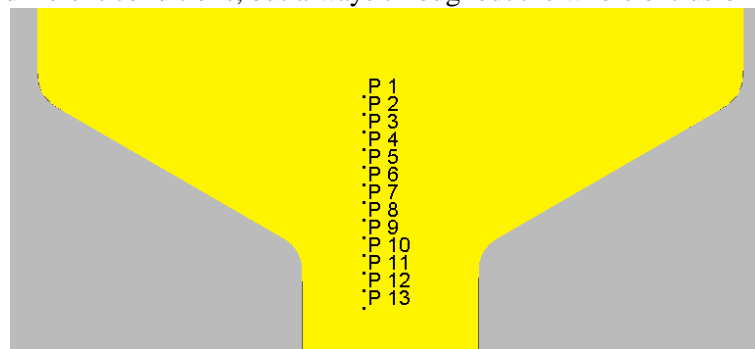


Figure 9. Deformation zone and the points for extracting deformation values ($d_{1-13}=12\text{mm}$)

The temperatures of the tracked points in deformation region of MISC composites under different conditions were exhibited in Figure 10. It can be seen that the temperatures of material increase significantly with the increase of extrusion ratio and speed and reach a peak near the outlet, i.e. the position of maximum strain. And the temperatures increase slowly along the line from point 1 to point 12 with a relative small extrusion ratio ($r<16$) and this also illustrated the uniform distribution of temperature of the workpiece. However, when extrusion ratio turns larger, the temperatures rise rapidly along the line (as shown in Figure 10(a)) due to the sharply increase of the effective strain

which will convert to heat. It can be noted the temperatures only have a little increase when the extrusion speed reaches a certain value ($v > 3\text{mm/s}$) as shown in Figure 10(b). Figure 11 shows the simulated strain rate of material in deformation zone along the extrusion direction. It can be seen that the strain rates also increase with extrusion speed and ratio which are similar to the variation of temperature.

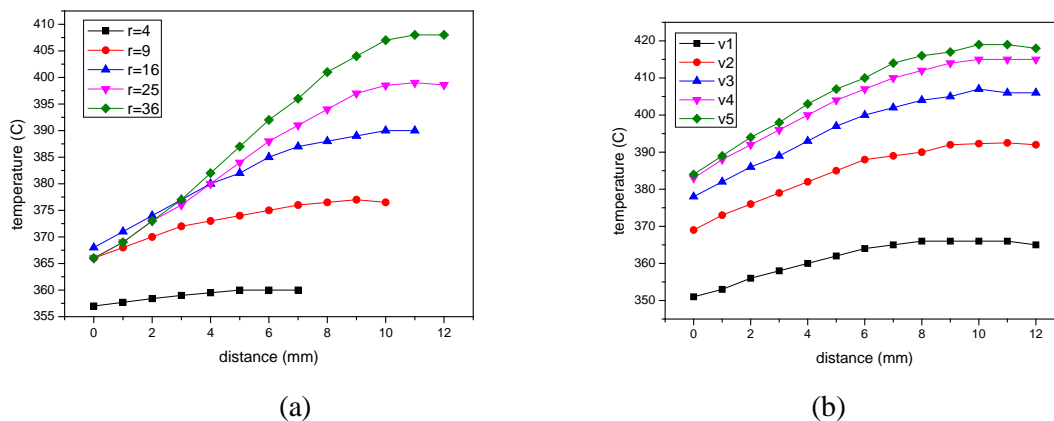


Figure 10. Simulated temperatures in deformation zone along the extrusion direction (a) at different extrusion speeds; (b) at different extrusion ratio

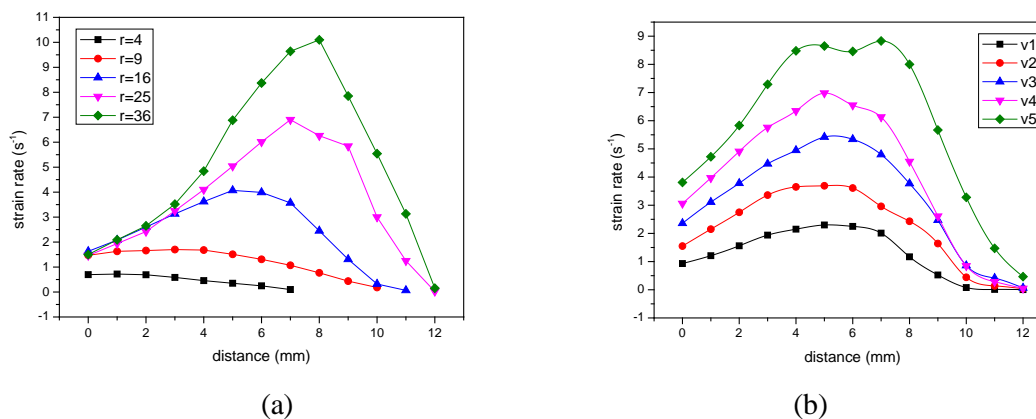


Figure 11. Simulated strain rate in deformation zone along the extrusion direction (a) at different extrusion speeds; (b) at different extrusion ratio

And the effective stresses of MISC material in deformation zone are directly related to the variations of its temperature and strain rate according to the flow stress equation as shown in Figure 12. The effective stress of the MISC workpiece increases continuously with the increase in extrusion ratio until it reaches a stable value when the extrusion ratio is too large ($r > 16$, as shown in Figure 12(a)). In contrast, the effective stress decreases with the increase in extrusion speed and reaches a stable value when $v > 2\text{mm/s}$ (as shown in Figure 12(b)). In conclusion, the effective stress would be influenced directly by the deformation temperatures and strain rate of material which affected by extrusion conditions, i.e. extrusion speed and ratio, and it increase with the increase in strain rate and the decrease in extrusion temperature.

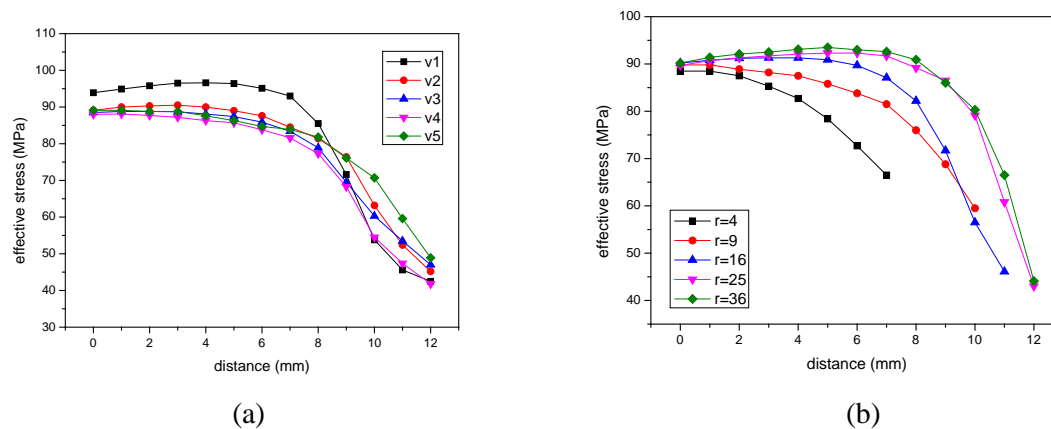


Figure 12. Simulated effective stress in deformation zone along the extrusion direction (a) at different ram speeds; (b) at different extrusion ratio

3.3.3. Extrusion pressure in relation with extrusion conditions.

Extrusion pressure changes with the displacement of extrusion head at different extrusion conditions are exhibited in Figure 13. It is observed that as a constant extrusion speed of 2mm/s, extrusion pressure is significantly increased with the increase of extrusion ratio (Figure 13(a)). So considering the workability and strength of the MISC material, especially the plasticity of magnesium matrix and the operability of the extrusion experiment, the extrusion ratio should not be chosen too large despite it can introduce greater stress. Generally the extrusion ratio can be selected as 16 to 25. Notably, the extrusion pressure is not affected obviously by extrusion speed when the extrusion ratio keep to a constant value of 16 as shown in Figure 13(b). So based on the previous analysis, a smaller extrusion speed can be chosen to enhance the effective stress when processing. And to ensure the efficiency, the extrusion speed should not be too small.

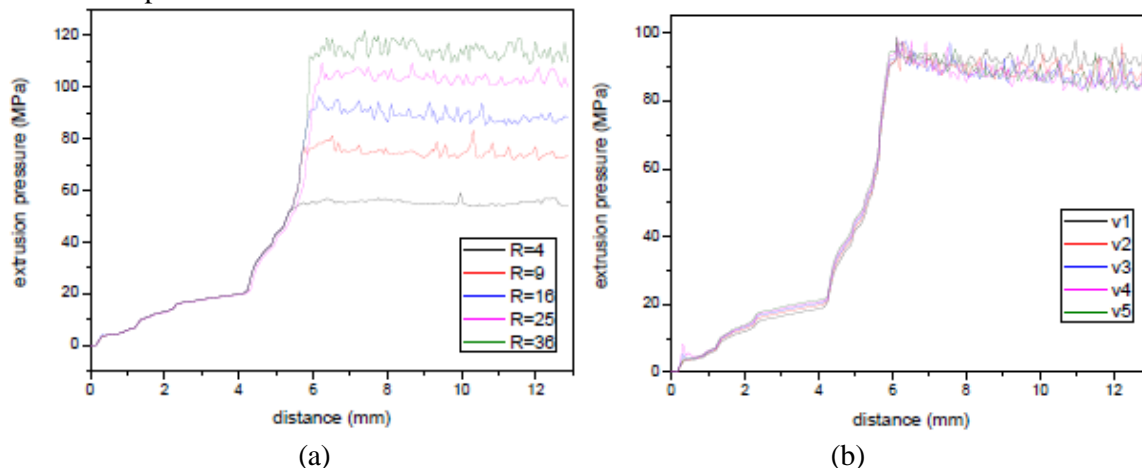


Figure 13. Extrusion pressure evolutions (a) at different extrusion ratio; (b) at different extrusion speed

4. Conclusions

1. One kind of interpenetrating magnesium composite reinforced by three-dimensional braided steel reinforcement (MISC composites) were constructed, and the microstructure characteristics of it in as-cast and as-extruded state were analyzed. The MISC composites in extruded state have much finer grains compared to the as-cast state and an improvement in mechanical properties compared to the Mg matrix material due to the effective load transfer from matrix to reinforcement and good interfacial bonding quality caused by extrusion.

2. The extrusion processes of MISC material were simulated by FE method. The flow of blank through the extrusion die can be divided into three steps: upsetting - filling of the extrusion chamber - continuous extruded according to the mesh characteristic and the evolution of extrusion pressure. And the combined quality between the reinforcement and matrix of MISC composites could be strengthened in the extrusion chamber where occurred large strain and suffered intense stress.
3. The effective stress of the MISC workpiece increases continuously with the increase in extrusion ratio and the decrease in extrusion speed until it reaches a stable value. And in order to acquire the larger effective stress so as to strengthen the bonding quality between Mg matrix and steel reinforcement, a appropriately high extrusion ratio and a low extrusion speed should be selected.

Acknowledgements

This work was supported by the National Natural Science Foundation of China (51372101) and the S&T Developing Program of Shandong Province, China (2016GGX103008, 2015GSF118016).

References

- [1] Wang S R, Song L H and Kang S K: Deformation behavior and microstructure evolution of wrought magnesium alloys, *Chinese Journal of Mechanical Engineering*, Vol. 26-3 (2013), p.437
- [2] Fletcher M, Siebert-Timmer A, Bichler L and Sediako D, Evolution of Strain and Microstructure During Creep of Wrought AE42 and ZE10 Magnesium Alloys, *Transactions of the Indian Institute of Metals* , Vol. 66-2(2013), p. 133
- [3] Alan A. Luo and Anil K. Sachdev: Development of a New Wrought Magnesium-Aluminum-Manganese Alloy AM30, *Metallurgical and Materials Transactions A* ,Vol. 38-6 (2007), p. 1184
- [4] Zhang X L , Chen G and Du Y L : Synthesis of Plastic Mg-Based Bulk-Metallic-Glass Matrix Composites by Bridgman Solidification, *Metallurgical and Materials Transactions A*,Vol. 43-8(2002), p. 2604
- [5] Varin R A: Intermetallic-reinforced light-metal matrix in-situ composites, *Metallurgical and Materials Transactions A*, Vol. 33-1 (2002), p. 193
- [6] Wang S R, Guo P Q, Yang L Y and Wang Y J: Microstructure and mechanical properties of AZ91 alloys by addition of rare earth yttrium, *Journal of materials engineering and performance*, Vol. 6 (2008), p.13
- [7] Wang S R, Wang Y, Li C C, Chi Q and Fei Z Y: The dry sliding wear behavior of interpenetrating titanium trialuminide /Aluminium composites, *Applied Composite Materials*, Vol. 14 (2007), p. 129
- [8] Wang S R, Kang S B, Cho J H and Wang Y J: Microstructure evolution of ZK60 magnesium alloy at CC/TRC/TRCHC processing following by annealing, *Transactions of Nonferrous Metals Society of China*, Vol. 20-5(2010),p.763
- [9] Shouren WANG, Wang M, Ma R, Wang Y and Wang Y J: Microstructure and hot compression behavior of twin-roll-casting AZ41M magnesium alloy, *Rare metals*, Vol. 29-4 (2010), p. 396
- [10] Palani swamy Hariharasudhan, Gracious Ngaile, Taylan Altan: Finite element simulation of magnesium alloy sheet forming at elevated temperatures, *Journal of Materials Processing Technology*; Vol. 146(2001), p.52
- [11] Wang S R, Guo P Q and Yang L Y: Deformation Behavior and Failure Analysis of Wrought Magnesium During Twin Rolling Casting and Hot Compression, *Journal of Engineering Materials and Technology*, Vol. 134(2012),p. 041002
- [12] Ma R, Wang S R, Wang Y and Yang L Y: Microstructure evolution of ZK60M twin-roll-casted magnesium alloy during hot compression and annealing, *Advance in materials research*, Vol. 284-286 (2011),p. 1502
- [13] Wang S R, Yang L Y, Ma R and Guo P Q: Fracture failure analysis of twin rolling casting magnesium by hot compression, *Advanced Materials Research* Vols. 123-125 (2010). P. 547